

Plasma Processing for Crystallization and Densification of Atomic Layer Deposition BaTiO₃ Thin Films

Jihwan An,^{*,†} Takane Usui,[†] Manca Logar,[‡] Joonsuk Park,[‡] Dickson Thian,[§] Sam Kim,^{||} Kihyun Kim,^{||} and Fritz B. Prinz^{†,‡}

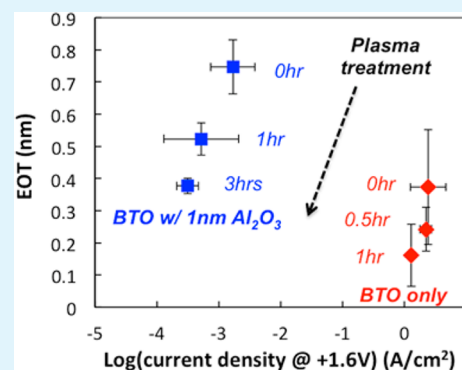
[†]Department of Mechanical Engineering, [‡]Department of Materials Science and Engineering, and [§]Department of Applied Physics, Stanford University, Stanford, California 94305, United States

^{||}Manufacturing Technology Center, Samsung Electronics, Suwon, Gyeonggi-Do, South Korea

S Supporting Information

ABSTRACT: High-*k*, low leakage thin films are crucial components for dynamic random access memory (DRAM) capacitors with high storage density and a long storage lifetime. In this work, we demonstrate a method to increase the dielectric constant and decrease the leakage current density of atomic layer deposited BaTiO₃ thin films at low process temperature (250 °C) using postdeposition remote oxygen plasma treatment. The dielectric constant increased from 51 (as-deposited) to 122 (plasma-treated), and the leakage current density decreased by 1 order of magnitude. We ascribe such improvements to the crystallization and densification of the film induced by high-energy ion bombardments on the film surface during the plasma treatment. Plasma-induced crystallization presented in this work may have an immediate impact on fabricating and manufacturing DRAM capacitors due to its simplicity and compatibility with industrial standard thin film processes.

KEYWORDS: atomic layer deposition, DRAM, BaTiO₃, remote plasma, crystallization



INTRODUCTION

Dynamic random access memories (DRAMs) are widely used for computer memory due to their simple structure, which consists of one transistor and one capacitor.^{1,2} For high charge storage density and a long storage lifetime, it is important for the dielectric film of the capacitor in DRAM to be (1) high-*k* (high dielectric constant), (2) ultrathin, (3) electrically insulating, and (4) conformal over high aspect ratio structures. In this regard, the use of atomic layer deposition (ALD) is essential in fabricating high quality DRAM capacitors because high-*k* thin films by ALD are known to be conformal over complex 3D structures and the thickness of the film can be accurately controlled down to the subnanometer range.^{3,4} Among high-*k* materials, perovskite materials, e.g., BaTiO₃ (BTO),^{5–7} SrTiO₃ (STO),^{2,5,6,8} or (Ba,Sr)TiO₃ (BST),^{9,10} are especially interesting due to their high dielectric constants (>100), even in thin films.

As-deposited ALD films are known to be amorphous due to their relatively low process temperature (usually <400 °C). The lack of crystallinity results in much lower dielectric constants than that of their single-crystalline counterpart. Therefore, extensive efforts have been made to crystallize the as-deposited amorphous ALD film using various in-situ or ex-situ techniques such as seed-layering^{1,2} or thermal annealing.⁵ These techniques, however, often need a high process temperature (>500 °C), which exceeds the acceptable thermal budget of DRAMs.

Crystallization by a plasma treatment is advantageous in that it does not need an elevated temperature; rather, the film is crystallized by the kinetic energy of ions transferred to the film surface by ion bombardment.¹³ Two major types of plasma have been employed for thin film crystallization: direct plasma and remote plasma. In direct plasma, the flux of ions and radicals is high as the plasma is formed at a close distance to the substrate. Therefore, the film can be effectively crystallized in situ, but it may be damaged by the plasma.¹⁴ In contrast, in remote plasma, the plasma source is located further away from the substrate. Hence, it has a lower flux of ions than direct plasma does, e.g., $\sim 10^{13}$ cm⁻² s⁻¹ for direct plasma (capacitive-coupling plasma) and $\sim 10^{12}$ cm⁻² s⁻¹ for remote plasma (inductively coupled plasma) at 200 mTorr,^{30,31} which may minimize the damage of the film by the plasma. Due to the low ion density, however, crystallizing a film with remote plasma is known to be challenging.^{13,14}

In this report, we show that ALD BaTiO₃ thin films were crystallized and densified by a remote oxygen plasma treatment after deposition, in spite of the presumably low ion density. Consequently, both the dielectric constant and the leakage current density of the film improved. Considering that the remote plasma configuration used in our experiments can be

Received: April 20, 2014

Accepted: June 19, 2014

Published: June 19, 2014

readily employed in the current standard thin film fabrication processes, the findings presented here may have a significant implication in fabricating and manufacturing high- k thin films for high storage density capacitors for next generation DRAMs.

EXPERIMENTAL SECTION

Two different sets of samples were prepared in this experiment. One set had only BTO and the other set had BTO along with an Al_2O_3 layer at the bottom for reducing the leakage current (Figure 1b and 1c). The films were deposited on top of double-side polished Si wafers with high boron doping of 10^{19} cm^{-3} and a resistivity of $0.008 \Omega\text{-cm}$ as conductive substrates. An ohmic contact was fabricated on the back (cathode) side by sputtering aluminum and annealing in 20% H_2 and 80% N_2 at 450°C .

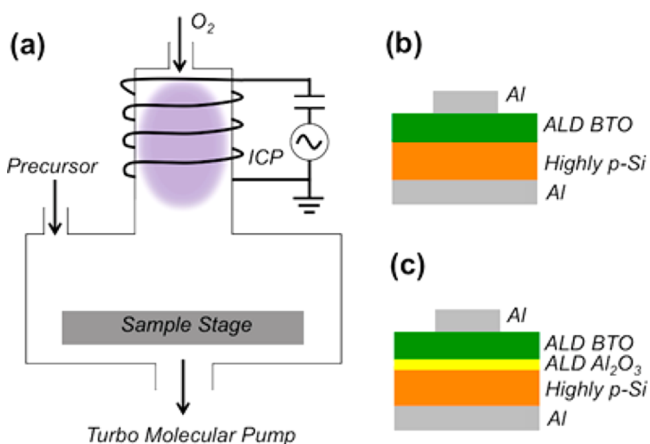


Figure 1. (a) Schematic of the ALD reactor with a remote plasma system.¹³ Structures of (b) BTO-only sample and (c) BTO with Al_2O_3 sample.

ALD BTO was grown by alternately depositing BaO and TiO_2 in our customized traveling wave type reactor as previously reported.¹⁵ Bis(propyl-tetramethyl cyclopentadienyl)barium (Alfa Aesar) was used as a Ba precursor, and titanium-tetraisopropoxide (TTIP) (Alfa Aesar) was used as a Ti precursor. Water was used as an oxidant. The Ba precursor was kept at 200°C and TTIP at 60°C . The substrate temperature was 250°C , which is inside the reported ALD windows of BaO and TiO_2 with precursor/oxidant combinations stated above.^{15,16} The BaO to TiO_2 pulse ratio was 1:1, in which one BaO cycle and one TiO_2 cycle constituted 1 supercycle. The growth rate was $0.5 \text{ \AA}/\text{supercycle}$. The X-ray photoelectron spectroscopy (XPS) (SSI S-probe) analysis showed that Ba to Ti ratio inside the film is 1 to 1.2, which is slightly Ti-rich compared to a stoichiometric cation ratio in BaTiO_3 (Figure S1a). No carbon peak was observable ($<0.1\%$) in the XPS spectra (Figure S1b).

We adopted an ultrathin blocking layer of PEALD Al_2O_3 (10 cycles, 1 nm in thickness) for the leakage current suppression between BTO (5 nm) and Si substrate (Figure S2). For Al_2O_3 deposition, we used the plasma-enhanced ALD reactor (FlexAL) by Oxford Instruments. Trimethylaluminum (TMA) was used as an Al precursor, and remote oxygen plasma (250 W, 15 mTorr) was used for oxidation (Figure 1a). The substrate temperature was 250°C . The growth rate of Al_2O_3 was $\sim 1 \text{ \AA}/\text{cycle}$. The plasma exposure time was 3 s, and the substrate temperature was 250°C .

After the deposition, samples were treated with the remote oxygen plasma (250 W, 15 mTorr) at 250°C in the PEALD station. After the plasma treatment, 200 nm of patterned top electrodes (anodes) of Al were deposited by DC sputtering. The top electrode area was $750 \mu\text{m} \times 750 \mu\text{m}$.

For the microstructural and compositional characterization of the film, transmission electron microscopy (TEM) and scanning TEM-electron energy dispersive spectroscopy (STEM-EDS) were used at

200 kV. For thickness, density, and roughness characterization, the X-ray reflectivity (XRR) was used (X'Pert Pro, PANalytical). For roughness characterization, atomic force microscopy (AFM) was used (JEOL S200). The equivalent oxide thicknesses (EOTs), i.e. $t_{\text{high-}k}(k_{\text{SiO}_2}/k_{\text{high-}k})$, and dielectric constants of ALD films were measured using LCR meter (Agilent, model no. E4980A). Current–voltage (i – V) measurements were taken using a Keithley 2636A SourceMeter as a voltage source and ammeter. The leakage currents were measured under +0 to +2 V bias.

The native SiO_2 layer on the Si electrode was assumed to form a series circuit with the ALD layer, and therefore its EOT, measured to be 23.9 \AA from a sample without an ALD layer, was subtracted from the total EOT. Because the Si electrode was extremely highly doped, the resulting SiO_2 tended to be much less insulating compared to a normal thermal oxide with measured resistivities ranging from 10^6 to $10^8 \Omega\text{-cm}$; therefore its contribution to the i – V measurement was negligible.^{11,17}

RESULTS AND DISCUSSION

First, we demonstrate the effect of postdeposition remote oxygen plasma treatment on the crystallinity of the film. Figures 2a–f show the cross-sectional TEM images of as-deposited, 1-h

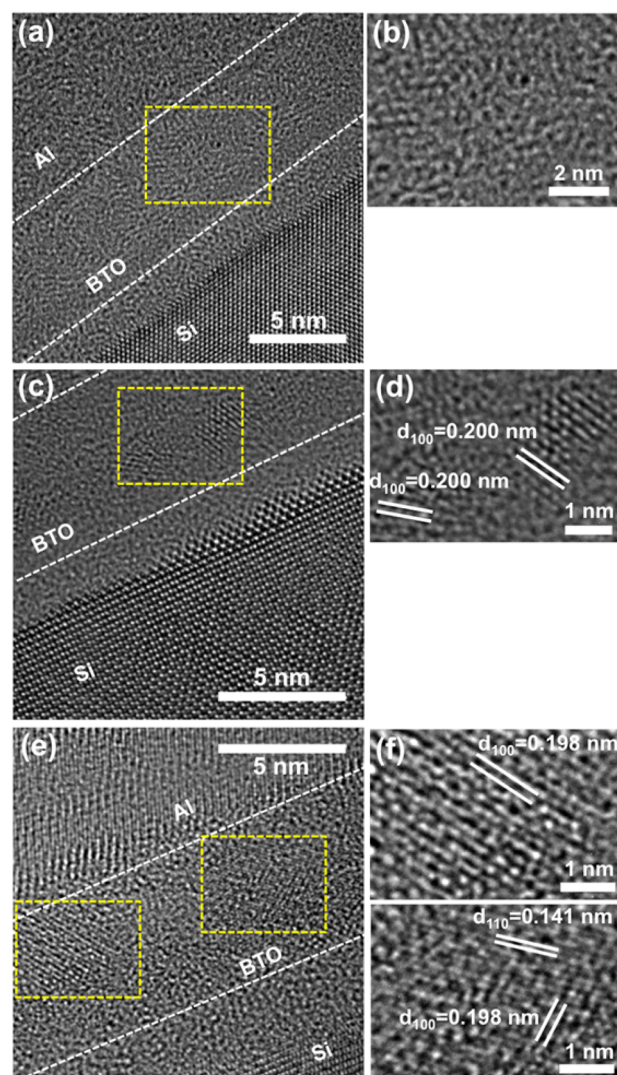


Figure 2. Cross-sectional TEM images of BTO (5 nm) samples; (a, c, and e) as-deposited, 1, and 3 h-treated samples, respectively; (b, d, and f) Zoomed-in images of the yellow boxes in parts a, c, and e, respectively.

treated, and 3-h treated BTO samples. As-deposited BTO film is completely amorphous as shown in Figure 2a and b. However, the 1- and 3-h treated films are shown to be partially crystallized (Figure 2c and e); 1–2 nm in size crystalline grains (1.8 ± 0.3 nm) are clearly shown in the 1 h-treated sample (Figure 2d) and grains of 3–5 nm (4.1 ± 0.5 nm) are observed in the 3 h-treated sample (Figure 2f). Lattice spacings in the crystalline area are measured at 0.198–0.200 and 0.141 nm. These values correspond well to (100) and (110) directions of cubic (a 0.394–0.403 nm), tetragonal (a 0.394–0.399 nm, c 0.399–0.404 nm), or rhombohedral (a 0.400 nm, θ 89.5°) BTOs,¹⁸ which implies the formation of single- or multiphase crystalline BTOs in the film.

It is notable that the crystallization of our BTO films occurred at a relatively low deposition temperature, i.e., 250 °C. The local temperature of the film surface during the plasma treatment does not change significantly, because gaseous species are not heated in cold plasmas.¹³ Instead, we speculate the energy provided by ion bombardments on the film surface may have been transferred into the film, helping crystalline grains to form.²⁹ The mean energy of ions in our experimental conditions, i.e., 250 W remote oxygen plasma at 15 mTorr, is known to be approximately 20 eV.¹³ Takagi et al. reported that ions within this energy range can displace the lattice atoms, while not sputtering them.¹⁹ Similar crystallization behavior in ALD films has been reported by Kim et al. for HfO₂ deposited using direct plasma ALD.¹⁴ Interestingly, in that same paper, the authors reported that the HfO₂ film deposited by remote plasma ALD was still amorphous, unlike our observations. This discrepancy seems to stem from the difference in the ion energy needed for crystallizing different materials: crystallization of BTO may be energetically more favorable than that of HfO₂. It has been reported that the ratio between the melting point (T_m) and temperature at which the homogeneous nucleation rate becomes maximum (T_n), i.e., T_n/T_m , is constant at 0.56 for inorganic materials.²⁰ This implies the kinetic energy of ions necessary for BTO crystallization may be lower than that for HfO₂, due to the significantly lower melting point of BTO (1625 °C) than that of HfO₂ (2758 °C).

Figure 3a shows the raw data obtained from XRR, and Figure 3b shows the effect of the remote oxygen plasma treatment on the density and the thickness of the film. The density and thickness of the as-deposited film are 3.25 g/cm³ and 16.2 nm, respectively. When the films are treated with the remote plasma, however, the density increases while the thickness slightly decreases. The density of the film increases to 3.97 and to 4.14 g/cm³ after plasma treatments for 1 and 3 h, respectively. The thickness of the film monotonically decreases as the treatment duration increases; it decreases to 13.6 nm after a 3 h-treatment, which is 16% thinner than the as-deposited film. Also, the film roughness decreases as the films are treated longer with plasma (Figure 4): the roughness decreases from 2.55 nm (as-deposited) to 1.23 and 1.06 nm for 1 and 3 h-treated samples, respectively, when measured with XRR. It decreases from 0.63 ± 0.18 nm (as-deposited) to 0.45 ± 0.01 nm and 0.45 ± 0.02 nm for 1 and 3 h-treated samples, respectively, when measured with AFM.

Plasma-induced densification of thin films has been previously reported by several researchers;^{21,22} thin films shrink and become denser upon plasma exposure, which corresponds well to our observations. Sun et al. experimentally proved that the sealing-off of the nanopores inside the film account for the densification.²¹ However, that may not explain the increase of

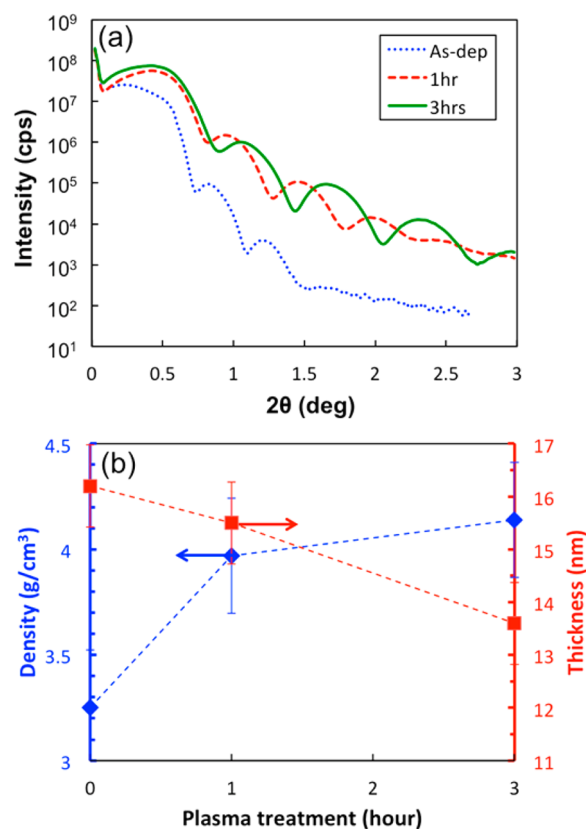


Figure 3. (a) X-ray reflectivity (XRR) spectra of BTO film: as-deposited, 1, and 3 h-plasma treated samples. (b) Density and thickness results derived from the XRR spectra.

density in our experiments considering the pinhole free nature of ALD films (see Figure 2a).³ We believe that the crystallization of the amorphous material is the main cause for the increased film density. Indeed, the density of BTO has been reported to increase as its crystallinity improves (amorphous 4.30 g/cm³, polycrystalline 5.61 g/cm³, single-crystal 6.02 g/cm³).²³ We attribute the smaller roughness of plasma-treated samples to the similar mechanism of what Sun et al. suggested: surface adatoms excited by ions have filled the surface pores, resulting in a smoother surface.

Changes in the physical properties induced by plasma treatment improve the electrical properties, e.g., the EOT and the leakage current density, of the films. The EOT of the as-deposited BTO-only film (5 nm) is 0.37 nm, and it decreases to 0.24 and 0.16 nm after 0.5 and 1 h/3 h-plasma treatments, respectively (Figure 5a). Corresponding dielectric constants are 51, 81, and 122 for as-deposited, 0.5, and 1 h/3 h-treated BTO samples, respectively. The dielectric constant of as-deposited BTO is lower than that reported for annealed ALD BTO (73–165 for films <100 nm) due to the mostly amorphous phase,^{5,7} the comparable dielectric constants of plasma-treated BTO to the reported values seem to stem from the crystallization. The dielectric constant of our plasma-treated BTO film is also still lower than that of thicker (>100 nm) BTO films,⁷ possibly due to the intrinsic dead-layer capacitance.²⁵ It is notable that the as-deposited BTO film shows relatively high dielectric constant compared to most of those for amorphous BTO films ($\epsilon \sim 9$ –43).^{7,26,27} We think that Ba–Ti–O chemical bondings in our BTO films may have been more complete compared to those in other amorphous films fabricated by physical vapor deposition

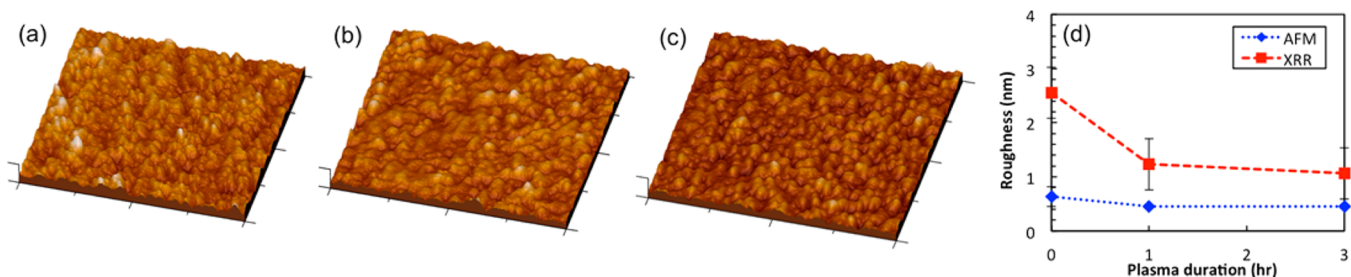


Figure 4. AFM images of BTO (16 nm-thick) samples: (a) as-deposited, (b) 1, and (c) 3 h-treated. Window sizes are 500 nm \times 500 nm, and Z-scales are identical at 6 nm. (d) Roughness measured with XRR (red square markers) and with AFM (blue diamond markers). The discrepancy between values from XRR and from AFM stems from the difference in the analyzed area size (XRR \sim cm \times cm, AFM \sim μ m \times μ m).

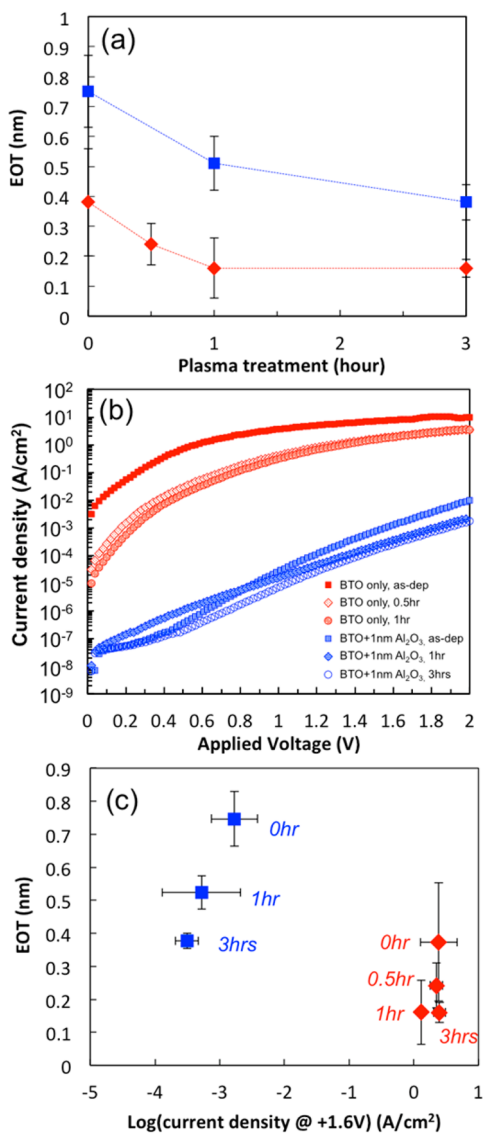


Figure 5. (a) EOT vs the duration of plasma treatment (red diamond markers BTO-only, blue square markers BTO with Al₂O₃), (b) the current density vs applied voltage with different plasma treatment conditions, and (c) EOT vs the leakage-current plot, of the 5 nm BTO-only (red diamond markers) and 5 nm BTO with 1 nm Al₂O₃ samples (blue square markers). The duration of each plasma treatment is shown next to markers. Leakage current density values were obtained at +1.6 V.

methods, which could cause a higher dielectric constant.²⁷ Also extremely small nucleates (1 nm or less in size) may have

formed even in the as-deposited film although they are not observed in the TEM images due to the mostly amorphous nature of the film. When compared to the dielectric constants of other ultrathin (<20 nm) high-*k* films ever reported, e.g., 108–210 for SrTiO₃,^{2,8,12,28} 83 for Al:TiO₂,¹ the observed dielectric constant for the 3 h-treated BTO film is one of the highest values. All the BTO-only films show a significant leakage current density of >1 A/cm² at +1.6 V (Figure 5b).

The EOT of the as-deposited BTO with 1 nm Al₂O₃ increases to 0.75 nm with the addition of 0.38 nm to that of the BTO-only film, which is reasonable considering the dielectric constant of PEALD Al₂O₃ (*k* \sim 8.6);²⁴ it decreases to 0.51 and 0.38 nm after 1 and 3 h-plasma treatments, respectively (Figure 5a). The leakage current density decreases by approximately one order after the plasma treatment for 3 h, down to 3×10^{-4} A/cm² at +1.6 V (Figure 5b).

Generally, the suppression of the leakage current is achieved at the expense of the increased EOT by an addition of a blocking layer, an increased physical thickness, or doping, for example.¹ In our observations, to the contrary, the plasma treatment decreases the EOT while simultaneously lowering the leakage current density, as clearly shown in Figure 5c. The plasma treatment improves the crystallinity and thereby increases the dielectric constant of BTO. At the same time, the treatment decreases the number of defects or vacancies in the film, which may have otherwise served as an electrical leakage path: the oxygen content inside the BTO film increased from 50% to 55% after plasma treatment for 3 h in XPS analysis. This result implies that the BTO film became more stoichiometric after the oxygen plasma treatment, which leads to a higher film density and lower leakage current.

CONCLUSION

ALD BTO thin films were grown at 250 °C on a highly doped-Si substrate and were post-treated with remote oxygen plasma. Plasma treatments for up to 3 h induced the crystallization of the films in approximately 4 nm grains. It also increased the film density by 27% after a 3 h-treatment, while slightly decreasing the thickness. The changes in electrical properties of BTO by plasma treatments were also investigated. With plasma treatments, the EOT of the film decreased while the leakage current also decreased. The dielectric constant of as-deposited 5 nm-thick BTO was 51, and it increased to 122 after a 1 h-plasma treatment. BTO with a 1 nm Al₂O₃ blocking layer with a 3 h-plasma treatment showed a small EOT (0.38 nm) with a relatively low leakage current density (3×10^{-4} A/cm² at +1.6 V). It should be noted, however, that these behaviors could be different if BTO films were deposited on other substrates, e.g., metallic substrates (Ru, TiN). Nevertheless, simultaneous

improvements of the EOT and the leakage current density from the use of plasma demonstrated in this work have a significant implication in fabricating and manufacturing capacitors with high storage density and long storage lifetime including DRAM applications.

■ ASSOCIATED CONTENT

5 Supporting Information

Supplementary figures, detailed descriptions of the sample preparation and the data postprocessing. This material is available free of charge via the Internet at <http://pubs.acs.org>.

■ AUTHOR INFORMATION

Corresponding Author

*E-mail: jihwanan@stanford.edu. Tel.: +1-650-724-6973. Fax: +1-650-723-5034.

Notes

The authors declare no competing financial interest.

■ ACKNOWLEDGMENTS

We thank the Manufacturing Technology Center, Samsung Electronics Co., Ltd., for financial support.

■ REFERENCES

- (1) Kim, S. K.; Choi, G.-J.; Lee, S. Y.; Seo, M.; Lee, S. W.; Han, J. H.; Ahn, H.-S.; Han, S.; Hwang, C. S. Al-Doped TiO₂ Films with Ultralow Leakage Currents for Next Generation DRAM Capacitors. *Adv. Mater.* **2008**, *20*, 1429–1435.
- (2) Lee, S. W.; Han, J. H.; Han, S.; Lee, W.; Jang, J. H.; Seo, M.; Kim, S. K.; Dussarrat, C.; Gatineau, J.; Min, Y.-S.; Hwang, C. S. Atomic Layer Deposition of SrTiO₃ Thin Films with Highly Enhanced Growth Rate for Ultrahigh Density Capacitors. *Chem. Mater.* **2011**, *23*, 2227–2236.
- (3) George, S. M. Atomic Layer Deposition: An Overview. *Chem. Rev.* **2010**, *110*, 111–131.
- (4) Matero, R.; Rahtu, A.; Haukka, S.; Tuominen, M.; Vehkamäki, M.; Hatanpää, T.; Ritala, M.; Leskelä, M. Scale-up of the BaTiO₃ ALD Process onto 200 mm Wafer. *ECS Trans.* **2006**, *1*, 137–141.
- (5) Vehkamäki, M.; Hatanpää, T.; Hänninen, T.; Ritala, M.; Leskelä, M. Growth of SrTiO₃ and BaTiO₃ Thin Films by Atomic Layer Deposition. *Electrochem. Solid-State Lett.* **1999**, *2*, S04–S06.
- (6) Wang, Z.; Yasuda, T.; Hatatani, S.; Oda, S. Enhanced Dielectric Properties in SrTiO₃/BaTiO₃ Strained Superlattice Structures Prepared by Atomic-Layer Metalorganic Chemical Vapor Deposition. *Jpn. J. Appl. Phys.* **1999**, *38*, 6817–6820.
- (7) Vehkamäki, M.; Hatanpää, T.; Ritala, M.; Leskelä, M.; Väyrynen, S.; Rauhala, E. Atomic Layer Deposition of BaTiO₃ Thin Films—Effect of Barium Hydroxide Formation. *Chem. Vap. Deposition* **2007**, *13*, 239–246.
- (8) Lee, S. W.; Kwon, O. S.; Han, J. H.; Hwang, C. S. Enhanced Electrical Properties of SrTiO₃ Thin Films Grown by Atomic Layer Deposition at High Temperature for Dynamic Random Access Memory Applications. *Appl. Phys. Lett.* **2008**, *92*, 222903–1–222903–3.
- (9) Schafraanek, R.; Gier, A.; Balogh, A. G.; Enz, T.; Zheng, Y.; Scheele, P.; Jakoby, R.; Klein, A. Influence of Sputter Deposition Parameters on the Properties of Tunable Barium Strontium Titanate Thin Films for Microwave Applications. *J. Eur. Ceram. Soc.* **2009**, *29*, 1433–1442.
- (10) Chen, B.; Yang, H.; Zhao, L.; Miao, J.; Xu, B.; Qiu, X. G.; Zhao, B. R.; Qi, X. Y.; Duan, X. F. Thickness and Dielectric Constant of Dead Layer in Pt/(Ba_{0.7}Sr_{0.3})TiO₃/YBa₂Cu₃O_{7-x} Capacitor. *Appl. Phys. Lett.* **2004**, *84*, S83–S85.
- (11) Usui, T.; Mollinger, S. A.; Iancu, A.; Reis, R. M.; Prinz, F. B. High Aspect Ratio and High Breakdown Strength Metal-Oxide Capacitors. *Appl. Phys. Lett.* **2012**, *101*, 033905–1–033905–4.

(12) Lee, W.; Han, J. H.; Jeon, W.; Yoo, Y. W.; Lee, S. W.; Kim, S. K.; Ko, C.-H.; Lansalot-Matras, C.; Hwang, C. S. Atomic Layer Deposition of SrTiO₃ Films with Cyclopentadienyl-Based Precursors for Metal–Insulator–Metal Capacitors. *Chem. Mater.* **2013**, *25*, 953–961.

(13) Profijt, H. B.; Potts, S. E.; van de Sanden, M. C. M.; Kessels, W. M. M. Plasma-Assisted Atomic Layer Deposition: Basics, Opportunities, and Challenges. *J. Vac. Sci. Technol. A* **2011**, *29*, 050801–1–050801–25.

(14) Kim, J.; Kim, S.; Jeon, H.; Cho, M.-H.; Chung, K.-B.; Bae, C. Characteristics of HfO₂ Thin Films Grown by Plasma Atomic Layer Deposition. *Appl. Phys. Lett.* **2005**, *87*, 053108–1–053108–3.

(15) Shim, J. H.; Park, J. S.; An, J.; Kang, S. K.; Gür, T. M.; Prinz, F. B. Intermediate-Temperature Ceramic Fuel Cells with Thin Film Yttrium-Doped Barium Zirconate Electrolytes. *Chem. Mater.* **2009**, *21*, 3290–3296.

(16) Xie, Q.; Musschoot, J.; Deduytsche, D.; Van Meirhaeghe, R. L.; Detavernier, C.; Van den Berghe, S.; Jiang, Y.-L.; Ru, G.-P.; Li, B.-Z.; Qu, X.-P. Growth Kinetics and Crystallization Behavior of TiO₂ Films Prepared by Plasma Enhanced Atomic Layer Deposition. *J. Electrochem. Soc.* **2008**, *155*, H688–H692.

(17) Usui, T.; Donnelly, C. A.; Logar, M.; Sinclair, R.; Schoonman, J.; Prinz, F. B. Approaching the Limits of Dielectric Breakdown for SiO₂ Films Deposited by Plasma-Enhanced Atomic Layer Deposition. *Acta Mater.* **2013**, *61*, 7660–7670.

(18) Wang, J. J.; Meng, F. Y.; Ma, X. Q.; Xu, M. X.; Chen, L. Q. Lattice, Elastic, Polarization, and Electrostrictive Properties of BaTiO₃ from First-Principles. *J. Appl. Phys.* **2010**, *108*, 034107–1–034107–6.

(19) Takagi, T. Ion–Surface Interactions during Thin Film Deposition. *J. Vac. Sci. Technol. A* **1984**, *2*, 382–388.

(20) Okui, N. Relationship between Crystallization Temperature and Melting Temperature in Crystalline Materials. *J. Mater. Sci.* **1990**, *25*, 1623–1631.

(21) Sun, J.-N.; Gidley, D. W.; Hu, Y.; Frieze, W. E.; Ryan, E. T. Depth-Profiling Plasma-Induced Densification of Porous Low-*k* Thin Films Using Positronium Annihilation Lifetime Spectroscopy. *Appl. Phys. Lett.* **2002**, *81*, 1447–1449.

(22) Ryan, E. T.; Martin, J.; Junker, K.; Wetzel, J.; Gidley, D. W.; Sun, J. N. Effect of Material Properties on Integration Damage in Organosilicate Glass Films. *J. Mater. Res.* **2001**, *16*, 3335–3338.

(23) Olson, J. C.; Stevison, D. F.; Bransky, I. The Effect of Temperature on Properties of RF Sputtered BaTiO₃ Films. *Ferroelectrics* **1981**, *37*, 685.

(24) Lim, J. W.; Yun, S. J. Electrical Properties of Alumina Films by Plasma-Enhanced Atomic Layer Deposition. *Electrochem. Solid-State Lett.* **2004**, *7*, F45–F48.

(25) Stengel, M.; Spaldin, N. A. Origin of the Dielectric Dead Layer in Nanoscale Capacitors. *Nature* **2006**, *443*, 679–682.

(26) Sreenivas, K.; Mansingh, A.; Sayer, M. Structural and Electrical Properties of RF Sputtered Amorphous Barium Titanate Thin Films. *J. Appl. Phys.* **1987**, *62*, 4475–4481.

(27) Li, P.; Lu, T. M.; Bakhru, H. High Charge Storage in Amorphous BaTiO₃ Thin Films. *Appl. Phys. Lett.* **1991**, *58*, 2639–2641.

(28) Popovici, M.; Van Elshocht, S.; Menou, N.; Swerts, J.; Pierreux, D.; Delabie, A.; Brijs, B.; Conard, T.; Opsomer, K.; Maes, J. W.; Wouters, D. J.; Kittl, J. A. Atomic Layer Deposition of Strontium Titanate Films Using Sr(^tBu₃Cp)₂ and Ti(OMe)₄. *J. Electrochem. Soc.* **2010**, *157*, G1–G6.

(29) Caturla, M. J.; de la Rubia, T. D.; Gilmer, G. H. Recrystallization of a Planar Amorphous–Crystalline Interface in Silicon by Low Energy Recoils: A Molecular Dynamics Study. *J. Appl. Phys.* **1995**, *77*, 3121–3125.

(30) Profijt, H. B.; Kessels, W. M. M. Ion Bombardment during Plasma-Assisted Atomic Layer Deposition. *ECS Trans.* **2013**, *50*, 23–34.

(31) Profijt, H. B.; Kudlacek, P.; van de Sander, M. C. M.; Kessels, W. M. M. Ion and Photon Surface Interaction during Remote Plasma ALD of Metal Oxides. *J. Electrochem. Soc.* **2011**, *158*, G88–G91.